The Nanoparticle-induced Zener Pinning Effect on Strain-softening in a Cold-Worked Cu-Al_2O_3 Composite with 0.1 wt.% Al Content

Dongping ZHANG [1, 2] *, Peng WEI [2], Hengju LI [2], Zhihui CHEN [3], Kuixian WEI [1]

[1] *Kunming University of Science and Technology, Kunming 650093, China*
[2] *Huanggang Polytechnic College, Huanggang 438002, China*
[3] *Shanghai Tianma Micro-Electronics Co., Ltd. Shanghai 201201, China*

http://doi.org/10.5755/j02.ms.36919

Received 8 April 2024; accepted 20 May 2024

The thermo-stability of microstructure during isothermal annealing at 900 °C and 1000 °C in a cold-worked Cu-Al_2O_3 composite with 0.1 wt.% Al content and its effect on resistance to softening were investigated in this paper. The results reveal that the microstructure following cold deformation consists of a Cu matrix with a refined grain size and high-density dislocations, accompanied by dispersed Al_2O_3 nanoparticles exhibiting an extremely low volume fraction. During isothermal annealing at 900 °C, the Al_2O_3 nanoparticles can strongly restrict the migration of the dislocations and suppress the recrystallization of the fine-grained Cu matrix by the Zener pinning effect. Furthermore, the presence of pinned dislocations facilitates the formation of sub-grain boundaries comprising high-density dislocations. Consequently, the Cu-Al_2O_3 composite with 0.1 wt.% Al content exhibits remarkable thermo-stability in its microstructure due to the incorporation of Al_2O_3 nanoparticles, resulting in a significantly elevated softening temperature of up to 1000 °C and thereby demonstrating excellent resistance against softening. However, the observed phenomenon of softening after isothermal annealing at 1000 °C for 5 hours can be attributed to extensive recrystallization growth that promotes twin boundary formation, primarily caused by the weakening Zener pinning effect resulting from Oswald ripening of Al_2O_3 and rod-like Al_2O_3 formation.

Keywords: work hardening, crystallographic texture, sub-grain boundary, recrystallization, random orientation, twin boundary.

1. INTRODUCTION

For alumina dispersion-strengthened copper (Cu-Al_2O_3 composite), the low deterioration of the dispersed Al_2O_3 particles has been adopted owing to its superior advantages such as high melting point, high hardness, and excellent thermo-stability and chemical inertness, on electrical and thermal conductivities of the pure Cu matrix due to low volume fraction favors the use of dispersion strengthening compared to solid solution strengthening, which significantly degrades these conductivities of copper. Furthermore, the oxide dispersion strengthening at elevated temperatures of the Cu-Al_2O_3 composite is stronger than the precipitate strengthening of the Cu-Cr, Cu-Ni-Si, and Cu-Cr-Zr alloys, since the coarsening of the sediments, residues that have lower thermo-stability compared to oxide particle [1 – 4]. It implies that the Cu-Al_2O_3 composite has good resistance to softening. Therefore, the Cu-Al_2O_3 composite with high strength and high conductivity is desirable for many industrial applications, such as resistance welding electrodes, high voltage breakers vacuum interrupters, connectors, and heat sinks [2 – 6].

However, successfully preparing a Cu-Al_2O_3 composite with high strength and high conductivity remains a challenge. A preparation process called internal oxidation combined with hot extrusion is generally considered to be an advanced technology for preparing the Cu-Al_2O_3 composite [7, 8]. The resulting microstructure comprises a Cu matrix with a refined grain size, accompanied by finely dispersed nanoparticles of Al_2O_3, as anticipated. However, the grain growth and the particle coarsening at elevated temperatures lead to deterioration of the mechanical strength, resulting from weakening grain boundary strengthening and dispersion strengthening. The achievement of a comprehensive understanding of the mechanisms governing microstructural stability and resistance to softening at elevated temperatures in the Cu-Al_2O_3 composite is therefore crucial.

Previous studies [1, 4, 7, 9, 10] have shown the stability of microstructure and mechanical properties at elevated temperatures of Cu- Al_2O_3 composites. For instance, Xiang et al. [1] have suggested that Cu-2.7 vol.% Al_2O_3 composite has high mechanical strength at elevated temperatures, which is attributed to the strong pinning effects of Al_2O_3 particles on the grain and sub-grain boundaries. Naser et al. [9] have concluded that for a Cu-3 vol.% Al_2O_3 composite, the presence of 3 vol.% Al_2O_3 particle in the Cu matrix results in the softening temperature of microstructure improved to 750 °C. Zhou et al. [10] have obtained that the ultrafine-structured Cu matrix in a Cu-5 vol.% Al_2O_3 composite is thermally very stable, suggesting a strong retarding effect of Al_2O_3 particles on the migration of grain boundaries. The resulting softening temperature reaches up to 900 °C and consequently, the softening phenomenon

* Corresponding author. Tel.: +86-151-72438252.
E-mail: *zhangdongping@hgpu.edu.cn* (D. Zhang)

occurs at higher temperatures, which is associated with the volume fraction reduction of Al_2O_3 particles with sizes in the range of 5 ~ 20 nm. However, Afshar et al. [7] have reported that abnormal grain growth via a mechanism analogous to that of site-saturated phase transformation occurs in a Cu-2.7 vol.% Al_2O_3 (15 nm) composite, resulting from an inhomogeneous size distribution of Al_2O_3 particles. These results have concluded that the uniform distribution of Al_2O_3 particles and the homogeneous distribution of these particles size are responsible for the high microstructure stability of microstructure and high mechanical properties at elevated temperatures in the Cu-Al_2O_3 composite.

During the internal oxidation combined with hot extrusion, however, the Al content of Cu-Al alloy powders could influence particle homogeneity and size distribution of Al_2O_3 precipitated by the internal oxidation process. Yet, both of that affect the microstructural thermo-stability of the Cu-Al_2O_3 composite. However, there has been limited research conducted on the thermo-stability of microstructure and its resistance to softening in the Cu-Al_2O_3 composite with an extremely low Al content. The present study investigates the thermo-stability of microstructure and its resistance to softening during isothermal annealing at high temperatures (such as 900 °C and 1000 °C) in a Cu-Al_2O_3 composite with an Al content of 0.1 wt.%.

2. EXPERIMENTAL DETAILS

A Cu-Al_2O_3 composite with 0.1 wt.% Al content that was investigated in this work was produced by internal oxidation combined with hot extrusion. For comparison, pure copper was also prepared via a similar route without performing the internal oxidation process. Subsequent, cold work with moderate plastic deformation, for the hot-extruded bars with a diameter of 20 mm, was conducted by using continuous multi-pass rotary swaging technology at room temperature, forming cold-worked bars of 12 mm diameter. It was followed by isothermal annealing at 900 and 1000 °C. For convenience, the hot-extruded and cold-worked bars for the pure copper and studied Cu-Al_2O_3 composite were denoted HE-Cu and CW-Cu and HE and CW, respectively. Moreover, Axxx/y-Cu and Axxx/y represented the annealed bars of the pure copper and studied Cu-Al_2O_3 composite, respectively, at where the xxx and y is the temperature (°C) and holding time (hour) of isothermal annealing, respectively.

Microstructural characterization was carried out using electron backscattering diffraction (EBSD), transmission electron microscope (TEM), X-ray diffraction (XRD), and differential scanning calorimetry (DSC) techniques. EBSD scans were conducted using a TSCAN LYRA3 microscope equipped with an electron backscattering diffraction system at an acceleration voltage of 20 kV. The specimens for the EBSD scans were prepared by standard mechanical grinding and then polishing, where the final polishing was conducted using a 0.04 μm colloidal silica slurry. For TEM observation on a JEOL 2100F microscope operating at 200 kV, thin-foil specimens with a diameter of 3 mm and thickness of 0.2 mm were mechanically thinned to 50 μm using 4000 grit SiC paper and finally, ion thinned using a Gatan 691 ion thinner. X-ray diffraction (XRD) experiments were performed on a SmartLab III X-Ray Diffractometer employing Cu Kα radiation operating at 45 kV voltage and a tube current of 200 mA. The XRD spectrums were obtained using a scanning step size of 0.02° and a scanning speed of 2° minute-1. These spectrums were used for calculating of dislocation density with the equations shown in Ref. [11]. The specimens for the XRD experiments were metallographically polished and then etched in hydrochloric acid for 30 secconds in order to minimize the possible errors originating from the polishing process. Differential scanning calorimetry (DSC) experiments were performed using a 96Line Calorimeter. The DSC curves were obtained using heating rates of 5 K/min and 10 K/min and a cooling rate of 10 K/min between 50 °C and 1000 °C. High-purity argon gas was used to protect the specimens from oxidation during thermal scanning. The specimens with a diameter of 6 mm and length of 20 mm for the DSC experiments were cleaned in a 3 % HNO_3 solution to eliminate oxides and contamination.

Vickers hardness (HV) was measured using an FM300 micro-hardness tester equipped with a Vickers indenter. Each hardness indentation was performed using a load of 200 g applied for 10 s dwell time on the well-polished surface of specimens. The mechanical strength was evaluated by conducting tensile tests. The tensile tests were carried out using a Zwick/Roell Z100 mechanical testing device with a constant strain rate of 4.0×10^{-3} s-1 at room temperature. The tensile specimens were nominally 6 mm in diameter with a gauge length of 30 mm. In all tensile tests, the loading direction was aligned with the axial direction of the bars.

3. RESULTS

3.1. Mechanical properties

The measured Vickers hardness (HV) values of the pure copper and studied Cu-Al_2O_3 composite are summarized in Table 1. The hardness of the HE sample was significantly higher than that of the HE-Cu sample. This implies that the presence of Al_2O_3 in the pure Cu matrix was conducive to improve the hardness of the studied Cu-Al_2O_3 composite compared to the pure copper.

Table 1. Determined hardness and yield strength (YS), ultimate tensile strength (UTS), and plastic strain to fracture (PSF) of tensile tests for the pure copper and studied Cu-Al_2O_3 composite

Sample code	HE-Cu	HE	CW	A900/1	A900/5	A1000/1
Hardness, HV0.2	59±2	114±3	133±2	119±3	117±2	116±2
YS, MPa	84±13	279±8	435±10	340±5	336±5	327±5
UTS, MPa	228±15	351±12	451±8	399±5	389±10	387±5
PSF, %	58±2	28±2	11±2	19±2	27±2	19±2

Moreover, the CW sample had the highest hardness, resulting from the hardness improved by the cold work with moderate plastic deformation and then decreased by the isothermal annealing at high temperatures.

However, the hardness of the A1000/1 sample was slightly higher than that of the HE sample. These results

indicate that the studied Cu-Al_2O_3 composite exhibited better cold work hardening capacity and good resistance to softening during the isothermal annealing at high temperatures. Fig. 1 shows engineering tensile stress-strain curves of the studied Cu-Al_2O_3 composite.

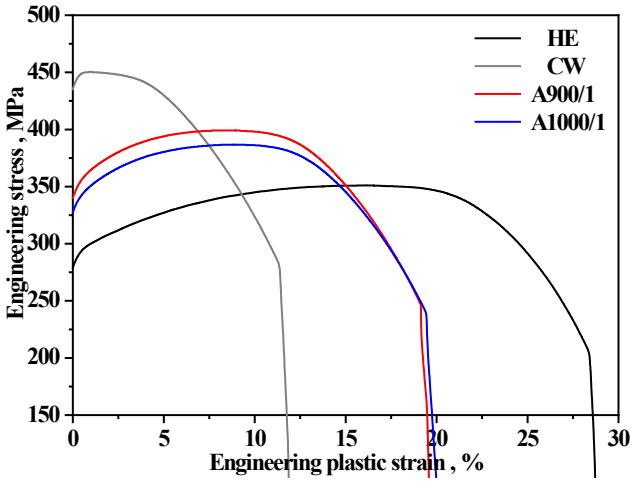

Fig. 1. Engineering tensile stress-strain curves of the studied Cu-Al_2O_3 composite.

The obtained tensile properties containing yield strength (YS), ultimate tensile strength (UTS), and plastic strain to fracture (PSF) are summarized in Table 1. The HE sample had an excellent combination of tensile strength and plasticity, where the YS, UTS, and PSF were determined to be 279 ± 15 MPa, 351 ± 20 MPa, and 28 ± 5 %, respectively. After the cold work, the YS and UST increased to 435 ± 5 MPa and 451 ± 5 MPa, respectively, while the PSF decreased to 11 ± 2 %. On the contrary, both the reduction of the YS and UST and the increment of the PSF occurred after the isothermal annealing at high temperatures. The isothermal annealing at high temperatures resulted in both a decrease in the YS and UST, as well as an increase in the PSF. Therefore, the tensile strength and plasticity of the studied Cu-Al_2O_3 composite could be regulated reasonably by cold work with moderate plastic deformation and then isothermal annealing at high temperature. After the cold work followed by isothermal annealing at 900 °C for 5 hours, the studied Cu-Al_2O_3 composite could obtain an outstanding combination of tensile strength and plasticity, which was evidenced by the tensile strength of 390 MPa and PSF of 27 %.

3.2. Microstructure

Microstructural TEM images of the HE sample are shown in Fig. 2. It reveals that the Cu matrix contained fine-sized Cu grains with an equiaxed structure (Fig. 2 a). Moreover, the dispersed nanoparticles with an ultra-low volume fraction could be observed from the fine-grained Cu matrix (Fig. 2 b). These particles on the grain boundaries or in the grains were inferred to be alumina (Al_2O_3) that was precipitated in-site by the internal oxidation process from Cu-0.1 wt.% Al alloy powders [12, 13]. As a result, for the studied Cu-Al_2O_3 composite, the microstructure after hot extrusion contained a fine-grained Cu matrix along with dispersed Al_2O_3 nanoparticles of an ultra-low volume fraction as expected. Fig. 3 shows EBSD-inverse pole figure (IPF) colouring images of the Cu grains for the HE and CW samples. The images demonstrate a uniform distribution of both the size and morphology of Cu grains through hot extrusion and cold work. As seen in Fig. 3 a, furthermore, it can be observed that the crystallographic orientations of the hot-extruded Cu grains were not complete random distribution [14]. Further analysis of the calculated IPF indicates the hot-extruded Cu grains had a crystallographic texture. After the cold work, however, the max experiment density for the calculated IPF was reached up to 22.1 from 3.6, as shown in Fig. 3. The measured average sizes of the Cu grains for the studied Cu-Al_2O_3 composite are summarized in Table 2, which were determined by circle equivalent diameter.

Table 2. Determined average sizes of the Cu grains and dislocation densities in the microstructures for the studied Cu-Al_2O_3 composite

Sample code	HE	CW	A900/1	A900/5	A1000/1	A1000/5
Average size, μm	0.84	0.59	0.67	0.70	0.88	1.2
Dislocation density, $\times 10^{14}$ m^{-2}	0.83	9.9	3.1	2.4	2.2	~

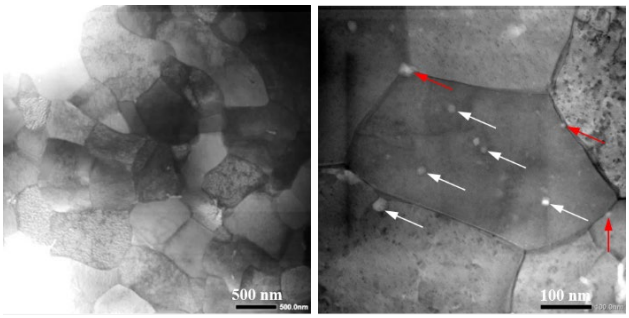

a b

Fig. 2. Microstructural TEM images of the HE sample: a – fine-sized Cu grains with an equiaxed structure; b – dispersed nanoparticles

The average sizes of the Cu grains for the HE and CW samples were determined to be 0.84 μm and 0.59 μm respectively. The results illustrate a significant enhancement in crystallographic texture due to cold work, accompanied by concurrent grain refinement.

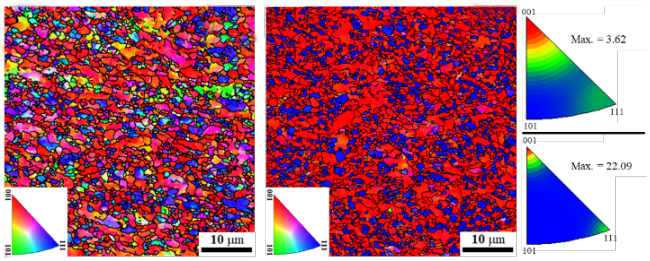

a b

Fig. 3. EBSD-inverse pole figure (IPF) coloring images: a – Cu grains for the HE; b – CW samples

EBSD-IPF coloring images of the Cu grains for the A900/1 and A1000/1 samples are shown in Fig. 4. It reveals that a small number of the Cu grains with random orientation were observed from the A900/1 sample (Fig. 4 a), while most of the Cu grains for the A1000/1 sample (Fig. b) had random orientation. EBSD-IPF coloring images of the Cu grains for the A900/1 and A1000/1

samples are shown in Fig. 4.

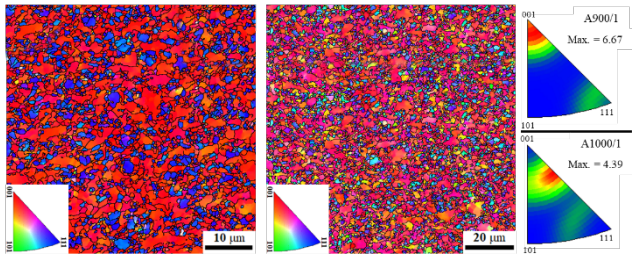

a b

Fig. 4. EBSD-IPF coloring images of the Cu grains: a – for the A900/1; b a – for the A1000/1 samples

It reveals that a small number of the Cu grains with random orientation were observed from the A900/1 sample (Fig. 4 a), while most of the Cu grains for the A1000/1 sample (Fig. 4 b) had random orientation. The formation of the randomly orientated Cu grains was inferred from recrystallization during the isothermal annealing at high temperatures. Therefore, the degree of recrystallization after isothermal annealing at 900 °C for 1 hour was lower than that at 1000 °C for 1 hour. Fig. 5 shows EBSD-IPF coloring images of the Cu grains and corresponding grain boundary images for the A900/5 and A1000/5 samples.

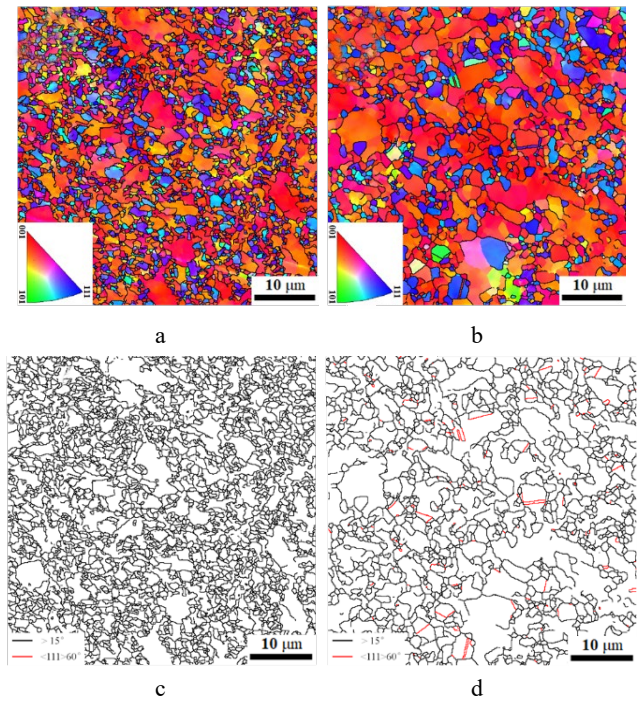

a b

c d

Fig. 5. a, b – EBSD-IPF coloring images; c, d – corresponding grain boundary images of the Cu grains for the A900/5 (a and c) and A1000/5 (b and d) samples

The coloring images (Fig. 5 a and b) reveal that the number of the randomly orientated Cu grains for the A900/5 sample remained very small compared to the A1000/5 sample. However, the twin boundaries associated with the recrystallization were only observed from the A1000/5 sample, as seen in Fig. 5 c and d. Furthermore, the average size of the Cu grains for the A900/5 sample was slightly larger than that for the A900/1 sample, while the A1000/1 and A1000/5 samples had significantly larger average sizes compared to the A900/1 and A900/5 samples, respectively, as listed in Table 2. These results demonstrate that the nucleation and growth of recrystallization were significantly suppressed during the isothermal annealing at 900 °C compared to 1000 °C. Therefore, the studied Cu-Al_2O_3 composite subjected to cold work had high thermo-stability of microstructure during the isothermal annealing at 900 °C, which will be discussed in the subsequent section.

4. DISCUSSION

4.1. High thermo-stability of fine-grained Cu matrix associated with the presence of Al_2O_3 nanoparticles

Fig. 6 shows the determined DSC curves at different heating rates of the studied Cu-Al_2O_3 composite subjected to cold work. Analysis of the DSC curves obtain the start temperatures of recrystallization were determined to be 990 ± 5 °C and 945 ± 5 °C at the heating rates of 5 K/min and 20 K/min, respectively, which was strongly dependent on the heating rate associated with decreasing dislocation and internal stress during the heating process.

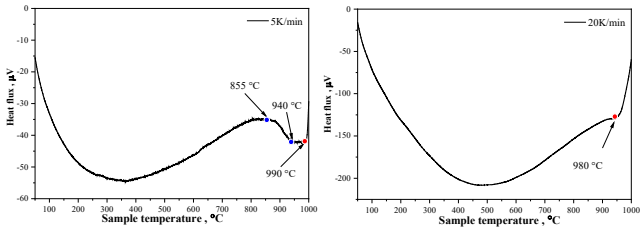

a b

Fig. 6. Determined DSC curves at heating rates of the CW sample: a – 5 K/min; b – 20 K/min

Therefore, the recrystallization degree after isothermal annealing at 1000 °C for 1 hour was higher than that at 900 °C for 1 hour, which could be evidenced by the microstructures of the A900/1 and A1000/1 samples (Fig. 4). EBSD-IPF colouring images of the Cu grains for the pure copper are shown in Fig. 7. After the cold work, the Cu grains without dispersed nanoparticles of Al_2O_3 (Al_2O_3-free Cu grains) reveal a mutually parallel lamellae structure along the deformation direction (Fig. 7 a). However, the lamellae structure for the Cu grains was completely transformed into an equiaxed structure during the isothermal annealing at 900 °C for 1 hour, as seen in Fig. 7 b. Furthermore, the equiaxed Cu grains possessed the characteristic of large sizes, random orientations, and twin boundaries. The results demonstrate that, for the cold-worked pure copper, the recrystallization occurred dramatically during the isothermal annealing at 900 °C for 1 hour, forming fully recrystallized Cu grains with an equiaxed structure and twin boundaries. Therefore, it is suggested that, after the isothermal annealing at 900 °C for 1 hour, the recrystallization degree of the cold-worked Cu-Al_2O_3 composite was significantly lower than that of the cold-worked pure copper, which could be attributed to the presence of the dispersed Al_2O_3 nanoparticles in the fine-grained Cu matrix (Fig. 2 b). This is explained by the fact that the migration of grain boundaries was significantly retarded by a very effective strong force from the dispersed

Al_2O_3 nanoparticles even at 900 °C, via the Zener pinning effect. Tian et al. [3] have suggested that the suppression of recrystallization for the Al_2O_3-dispersed Cu grains of Cu-Al_2O_3 composite could be related to the prolonged nuclei formation process utilizing sub-grains boundaries protruding mechanism and adjacent sub-grain merging mechanism.

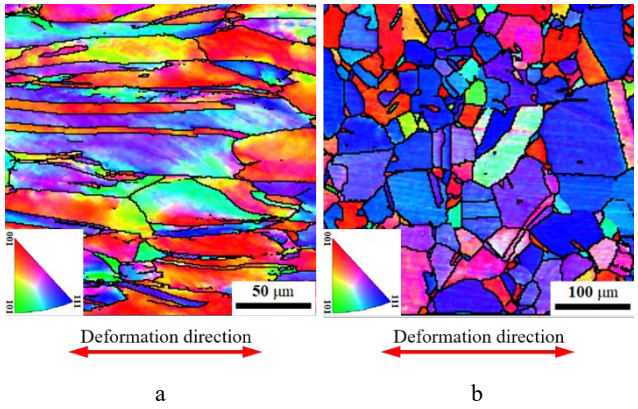

Fig. 7. EBSD-IPF coloring images of the Cu grains for the pure copper: a – CW-Cu sample; b – A900/1-Cu sample

Dislocation densities of the studied Cu-Al_2O_3 composite were calculated by analyzing their XRD spectrums. The calculated dislocation densities are summarized in Table 2. It indicates that the CW sample had the highest dislocation density. The dislocation density was significantly enhanced through cold work, followed by a subsequent reduction during isothermal annealing at elevated temperatures. However, the microstructure of the A1000/1 sample retained a high dislocation density compared to the HE sample. Therefore, it is suggested that the dislocations induced by cold work had high thermo-stability even at 1000 °C. High-resolution dislocation characteristics of the A1000/1 sample are shown in Fig. 8. This demonstrates the migration of dislocations during the isothermal annealing at 1000 °C was also inhibited significantly by the strong Zener pinning effect from the dispersed Al_2O_3 nanoparticles (Fig. 8 a).

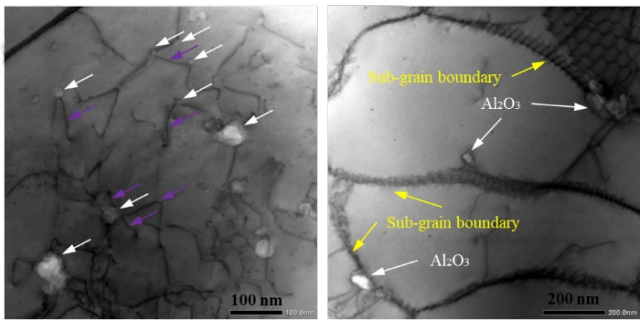

Fig. 8. Microstructural TEM images: a – A1000/1 sample, showing preventing dislocations; b – sub-grain boundaries with high-density dislocations by the strong Zener pinning effect from the dispersed Al_2O_3 nanoparticles

Furthermore, the dispersed Al_2O_3 nanoparticles in the grains facilitated the formation of sub-grain boundaries consisting of high-density dislocations (Fig. 8 b), which was associated with the Zener pinning effect from the interaction of the migration of dislocations with high density and the dispersed Al_2O_3 nanoparticles of high hardness. As a result, the presence of the dispersed Al_2O_3 nanoparticles not only on the grain boundaries but also in the grains was conductive to improve the thermo-stability of the microstructure.

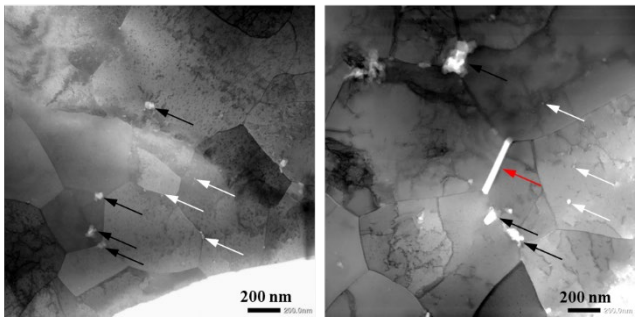

Fig. 9. Microstructural TEM images: a – A900/5 sample; b – A1000/5 sample, showing fine-sized (white arrow) and large-sized (black arrow) particles of Al_2O_3 as well as rob-liked (red arrow) Al_2O_3

It is well known that the Zener pinning effect for grain growth and dislocation migration from oxide particles is related to the effective diameter and distance of these particles [13]. To corroborate the Zener pinning effect from the dispersed particles of Al_2O_3 in the studied Cu-Al_2O_3 composite, high-resolution TEM images of the microstructures for the A900/5 and A1000/5 samples are shown in Fig. 9. It reveals the sizes of the dispersed Al_2O_3 particles remained in a range of 5 ~ 20 nm for the A900/5 sample (Fig. 9 a). However, both large-sized Al_2O_3 particles with an above 20 nm size and rod-liked Al_2O_3 were observed from the A1000/5 sample (Fig. 9 b). As deduced from the Zener pinning mechanism, the resistance to grain growth for the A1000/5 sample was weakened by increasing the effective diameter of Al_2O_3 particles and the distance between these particles, owing to the Oswald ripening of Al_2O_3 and the formation of rod-liked Al_2O_3 during the isothermal annealing at 1000 °C for 5 hours. Accordingly, it is demonstrated that the high thermo-stability of the fine-grained Cu matrix during the isothermal annealing at 900 °C was essentially dependent on the ultra-high thermo-stability of the dispersed Al_2O_3 nanoparticles.

4.2. Relationship between microstructural thermo-stability and resistance to softening

The softening temperature of Cu and Cu alloys is defined to the given temperature, at which a 15 % reduction in hardness or strength after isothermal annealing at the given temperature for 1 hour. Table 3 lists the calculated reduction fraction in hardness and UTS after isothermal annealing for the studied Cu-Al_2O_3 composite subjected to cold work. The reduction fractions in hardness and UTS for the A1000/1 sample were calculated to be 12.8 % and 14.4 %, respectively. Furthermore, the reduction fractions in hardness and UTS for the A9000/5 sample retained below 15 %. However, for the A1000/5 sample, the hardness reached up to 22 % decrement. As a result, the studied Cu-Al_2O_3 composite subjected to cold work had a high softening temperature reaching up to 1000 °C, while the softening phenomenon occurred after the isothermal annealing at 1000 °C for 5 hours.

Table 3. Calculated reduction fraction (%) in hardness and UTS after isothermal annealing at different temperatures for the studied Cu-Al_2O_3 composite subjected to cold work

Sample code	A900/1	A900/5	A1000/1	A1000/5
Hardness	10.5	12.0	12.8	26.3
UST	11.5	13.7	14.4	~

Therefore, it is suggested that the retaining fine-sized Cu grains (Fig. 2, Fig. 3, Fig. 4), sub-boundaries (Fig. 8), and high-density dislocations (Table 2) associated with the strong Zener pinning effect from the dispersed Al_2O_3 nanoparticles were responsible for the high softening temperature. However, the softening phenomenon that occurred after the isothermal annealing at 1000 °C for 5 hours was a consequence of the significant recrystallization growth for the Al_2O_3-dispersed Cu grains (Fig. 5 b and d), resulting from the weakening Zener pinning effect by the Oswald ripening of Al_2O_3 and the formation of rod-liked Al_2O_3 (Fig. 9 b). It is to be suggested that, therefore, the dispersed nanoparticles of Al_2O_3, for the studied Cu-Al_2O_3 composite, had effects of enhancing the resistance to softening by strong Zener pinning effect, increasing the mechanical strength by Orowan strengthening, and improving the work hardening capability by pinning mobile dislocations during plastic deformation [3, 4, 7, 9, 15].

5. CONCLUSIONS

A Cu-Al_2O_3 composite with 0.1 wt.% Al content produced by internal oxidation combined with hot extrusion was studied. After cold work with moderate plastic deformation, for the studied Cu-Al_2O_3 composite, the microstructure contained a fine-grained Cu matrix with high-density dislocations as well as texture structure and dispersed Al_2O_3 nanoparticles of an ultra-low volume fraction as expected. The thermo-stability of microstructure during isothermal annealing at 900 °C and 1000 °C in the studied Cu-Al_2O_3 composite subjected to cold work and its effect on resistance to softening were investigated in this work. The main results can be summarized as follows:

First, the dispersed Al_2O_3 nanoparticles during isothermal annealing at 900 °C strongly pin dislocations in the fine-grained Cu matrix, effectively inhibiting their movement and preventing recrystallization. This leads to the formation of sub-grain boundaries with high-density dislocations and imparts exceptional thermo-stability to the cold-worked Cu-Al_2O_3 composite, which shows excellent resistance to softening up to 1000 °C.

Second, the presence of dispersed Al_2O_3 nanoparticles, which are highly hard and thermally stable, contributes to the microstructure's high stability during isothermal annealing at 900 °C. However, the softening phenomenon observed after isothermal annealing at 1000 °C for 5 hours can be attributed to significant recrystallization growth that promotes twin boundary formation due to weakened Zener pinning caused by Oswald ripening of Al_2O_3 and the formation of rod-like Al_2O_3.

Finally, after undergoing cold work and subsequent isothermal annealing at 900 °C for 5 hours, the Cu-Al_2O_3 composite demonstrated an exceptional combination of tensile strength and plasticity. This was evidenced by a tensile strength of up to 390 MPa, accompanied by a significant plastic strain fraction (PSF) of 27 %. The superior performance can be attributed to the composite's enhanced hardening capacity through cold work and its ability to resist softening during high-temperature isothermal annealing.

Acknowledgments

The Fundamental Research Funds for the Guangdong Academy of Sciences (Grant no. 2020GDASYL-20200103133) is gratefully acknowledged.

REFERENCES

1. **Xiang, Z.Q., Li, Z., Lei, Q., Xiao, Z., Pang, Y.** High Temperature Mechanical Behavior of Alumina Dispersion Strengthened Copper Alloy with High Content of Alumina *Transactions of Nonferrous Metals Society of China* 25 (2) 2015: pp. 444 – 450. https://doi.org/10.1016/S1003-6326(15)63622-6
2. **Rajkovic, V., Bozic, D., Jovanovic, M.T.** Effects of Copper and Al_2O_3 Particles on Characteristics of Cu–Al_2O_3 Composites *Materials & Design* 31 (4) 2010: pp. 1962 – 1970. https://doi.org/10.1016/j.matdes.2009.10.037
3. **Tian, B., Liu, P., Song, K., Li, Y., Liu, Y., Ren, F., Su, J.** Microstructure and Properties at Elevated Temperature of a Nano-Al_2O_3 Particles Dispersion-Strengthened Copper Base Composite *Materials Science and Engineering: A* 705 2006: pp. 435 – 436. https://doi.org/10.1016/j.msea.2006.07.129
4. **Trojanová, Z., Ferkel, H., Lukáč, P., Naser, J., Riehemann, W.** Thermal Stability of Copper Reinforced by Nanoscaled and Microscaled Alumina Particles Investigated by Internal Friction *Scripta Materialia* 40 1999: pp. 1063 – 1069. https://doi.org/10.1016/S1359-6462(99)00070-6
5. **Sato, S., Hatano, T., Kuroda, T., Furuya, K., Hara, S., Enoeda, M., Takatsu, H.** Optimization of HIP Bonding Conditions for ITER Shielding Blanket/First Wall Made from Austenitic Stainless Steel and Dispersion Strengthened Copper Alloy *Journal of Nuclear Materials* 265 1998: pp. 258 – 263. https://doi.org/10.1016/S0022-3115(98)00360-2
6. **Pokrovsky, A.S., Fabritsiev, S.A., Edwards, D.J., Zinkle, S.J., Rowcliffe, A.F.** Effect of Neutron Dose and Irradiation Temperature on the Mechanical Properties and Structure of Dispersion Strengthened Copper Alloys *Journal of Nuclear Materials* 404 2000: pp. 283 – 287. https://doi.org/10.1016/S0022-3115(00)00226-9
7. **Afshar, A., Simchi, A.** Abnormal Grain Growth in Alumina Dispersion-Strengthened Copper Produced by an Internal Oxidation Process *Scripta Materialia* 58 2008: pp. 966 – 969. https://doi.org/10.1016/j.scriptamat.2008.01.029
8. **Daoud, A., Vogt, J.B., Charkaluk, E., Bouquerel, J., Zhang, L., Biasci, J.C.** Anisotropy Effects on the Tensile and Fatigue Behaviour of an Oxide Dispersion Strengthened Copper Alloy *Materials Science and Engineering: A* 534 2012: pp. 640 – 648. https://doi.org/10.1016/j.msea.2011.12.021

9. **Naser, J., Ferkel, H., Riehemann, W.** Grain Stabilisation of Copper with Nanoscaled Al_2O_3-Powder *Materials Science and Engineering: A* 470 1997: pp. 234 – 236. https://doi.org/10.1016/S0921-5093(97)00263-3
10. **Zhou, D., Zhang, D., Kong, C., Munroe, P., Torrens, R.** Grain and Nanoparticle Coarsening of an Ultrafine Structured Cu–5vol.%Al_2O_3 Nanocomposite during Isochronal Annealing *Journal of Alloys and Compounds* 642 2015: pp. 83 – 91. https://doi.org/10.1016/j.jallcom.2015.04.106
11. **Zeng, W., Xie, J., Zhou, D., Fu, Z., Zhang, D., Lavernia, E.J.** Bulk Cu-NbC Nanocomposites with High Strength and High Electrical Conductivity *Journal of Alloys and Compounds* 745 2018: pp. 55 – 62. https://doi.org/10.1016/j.jallcom.2018.02.215
12. **Song, K., Xing, J., Dong, Q., Liu, P., Tian, B., Cao, X.** Internal Oxidation of Dilute Cu–Al Alloy Powers with Oxidant of Cu_2O *Materials Science and Engineering: A* 380 2004: pp. 117 – 122. https://doi.org/10.1016/j.msea.2004.03.042
13. **Li, C., Xie, Y., Zhou, D., Zeng, W., Wang, J., Liang, J., Zhang, D.** A Novel Way for Fabricating Ultrafine Grained Cu-4.5 vol% Al_2O_3 Composite with High Strength and Electrical Conductivity *Materials Characterization* 155 2019: pp. 109775. https://doi.org/10.1016/j.matchar.2019.06.017
14. **Hansen, N., Ralph, B.** The Strain and Grain Size Dependence of the Flow Stress of Copper *Acta Metallurgica* 30 1982: pp. 411 – 417. https://doi.org/10.1016/0001-6160(82)90221-8
15. **Brimhall, J.L., Klein, M.J., Huggins, R.A.** Influence of a Finely Dispersed Second Phase on Recrystallization *Acta Metallurgica* 14 1966: pp. 459 – 466. https://doi.org/10.1016/0001-6160(66)90313-0